MEASURING 6LI(N,T) AND 10B(N,A) CROSS SECTIONS USING THE NIST ALPHA-GAMMA DEVICE

M.S. DEWEY, D.M. GILLIAM, AND J.S. NICO

Physics Laboratory, National Institute of Standards and Technology, Gaithersburg, MD 20899, USA

G.L. GREENE

Dept. of Physics, University of Tennessee/Physics Division, Oak Ridge National Laboratory, Knoxville, TN 37831, USA

A. LAPTEV

Department of Physics, Tulane University, New Orleans, LA 70118-5636, USA

A. YUE

Department of Physics, University of Tennessee, Knoxville, TN 37831, USA

The ^{6}Li(n,t) and ^{10}B(n,α) cross sections are important neutron cross section standards. Precise knowledge of these cross sections is essential because they are often used as reference standards for obtaining the neutron fluence in investigations of the properties of neutron-induced reactions and for accurate determination of neutron cross sections. They are also used for fluence determinations in neutron dosimetry as well as fundamental physics experiments. Most of the previous measurements of the ^{6}Li(n,t) and ^{10}B(n,α) cross sections were made in the neutron energy region above thermal and frequently measurements were done relative another reaction cross section. The only measurements in the meV energy region were limited to determinations from the difference between measurements of total and scattering cross sections or integral-type measurements. We report on an effort to carry out the first direct and absolute measurements of these cross sections using 3.3 meV monoenergetic neutrons. These measurements are absolute determinations that are not dependent on any cross section for fluence determination.

1 Introduction

1.1. *Motivation*

The ^{6}Li(n,t) and ^{10}B(n,α) cross sections are important neutron cross section standards in the energy range from thermal energy to 1 MeV [1]. Precise knowledge of these cross sections is very important because they are often used as reference standards and for accurate determinations of other neutron cross sections. Most of the previous measurements of the ^{6}Li(n,t) and ^{10}B(n,α) cross sections were made in the neutron energy region well above thermal. The only measurements in the meV energy region were limited to determinations from the difference between measurements of total and scattering cross sections (for ^{10}B [2]) or integral-type measurements (thermal energy values for both ^{6}Li and ^{10}B cases [3]).

Due to the lack of direct measurements, the existing evaluations of ^{6}Li(n,t) and ^{10}B(n,α) cross sections use absolute data [4,5] as well as the ratio of these cross sections [6] and ratios to other reaction cross sections, such as ^{235}U(n,f), ^{238}U(n,f), *etc*. Although the latest recommended values for the ^{6}Li(n,t) and ^{10}B(n,α) standard cross sections at thermal energy have uncertainties of 0.14% and 0.25% [1], respectively, the difference in the thermal cross sections between evaluations ENDF/B-VII.0 [4] and JENDL-3.3 [5] is 0.20% and 0.14%. In the evolution of the ENDF/B evaluation from version VI to VII these cross sections were changed 0.27% and 0.08%. Providing new high-precision absolute measurements close to thermal energy is critical for addressing these differences.

Another motivation for this work is the need to measure neutron fluence at the ±0.1% level in order to make a precise measurement of the neutron lifetime. One technique to measure the neutron lifetime involves absolute counting of protons from neutron decay while continuously monitoring the neutron fluence. In the most precise experiment to date, the uncertainty in the measurement was limited at the ±0.3% level by the ability to measure the neutron fluence [7,8]. One approach to address this limitation makes use of an electrical substitution radiometer that measures the absolute flux of a cold neutron beam based on neutron absorption in a ^{6}Li-rich metallic alloy [9]. This technique has been used with good results [10], but some question remains regarding a possible systematic effect from defect formation. The approach using the Alpha-Gamma device described here shows promise for improving the uncertainty to the desired level.

1.2. *Overview of the Technique*

The method to measure the ^{10}B or ^{6}Li cross section is based on relating the total rate of neutron events in the Alpha-Gamma device to a neutron flux monitor containing a deposit of known mass. The target in the monitor, and hence the cross section that one measures, is interchangeable and is designed to measure either the ^{10}B or ^{6}Li cross section. (In this paper, we concentrate on ^{6}Li although the techniques are similar.) The method requires that the neutron beam that traverses the flux monitor is also incident on the Alpha-Gamma device, as illustrated in Fig. 1. Using the measurements of the total neutron flux from the Alpha-Gamma device, the energy of the beam, and the efficiency of the flux monitor (i.e., areal density of ^{6}Li times the solid angle), one can directly extract the cross section of the deposit material.

The Alpha-Gamma device counts prompt gamma-rays that originate from neutron capture in a totally absorbing boron target [11]. The gamma-ray efficiency is known accurately through calibration in a separate measurement using a thin ^{10}B target and a standard alpha-emitting source. In this manner, one establishes absolute counting without reference to either the boron target mass or the ^{10}B reaction cross section. The comparison of the flux from the Alpha-Gamma device with that from a second thin-target flux monitor whose geometry and target mass are both well known yields the ^{6}Li (or ^{10}B)

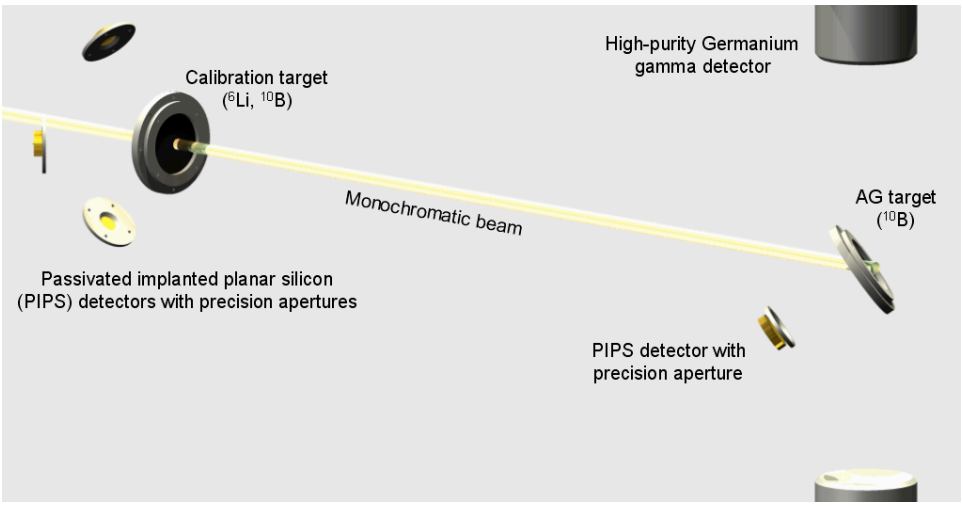

Figure 1. Schematic illustration of the alpha-gamma technique. A highly collimated monochromatic neutron beam passes through a thin target surrounded by 4 silicon detectors with precision apertures. It is then incident on a totally absorbing ^{10}B deposit and the resulting gamma and alpha particles are detected. Both detectors share a common vacuum system.

standard cross section measured at near-thermal neutron energy. This procedure should be capable of achieving an accuracy of ± 0.25%, where the limiting uncertainty is the knowledge of the deposit mass. The apparatus has been operated on one previous occasion to measure the absolute flux of a cold neutron beam at the 0.5% level [12].

2 Experimental Apparatus

2.1 Cold Neutron Beamline

The measurement is being performed using a monochromatic beam of cold neutrons at the National Institute of Standards and Technology Center for Neutron Research (NCNR). Neutron guides transport the cold neutrons reactor to the experimental area at the end of neutron guide 6 (NG-6) [13] in the NCNR Guide Hall. A pyrolytic graphite monochromator positioned in the beam Bragg reflects neutrons of approximately 0.5 nm to the beamline NG-6m. The beam traverses a He-filled flight tube and is collimated by two ^{6}LiF apertures before entering the vacuum chamber common to the neutron flux monitor and Alpha-Gamma device.

Precise knowledge of the energy of the neutron beam is necessary for determining the cross sections, so several measurements of the beam wavelength have been performed. The wavelength is determined by Bragg reflection from a perfect crystal silicon analyzer; extensive measurements and modeling were performed to measure the wavelength [14]. Previous measurements were performed with uncertainties below

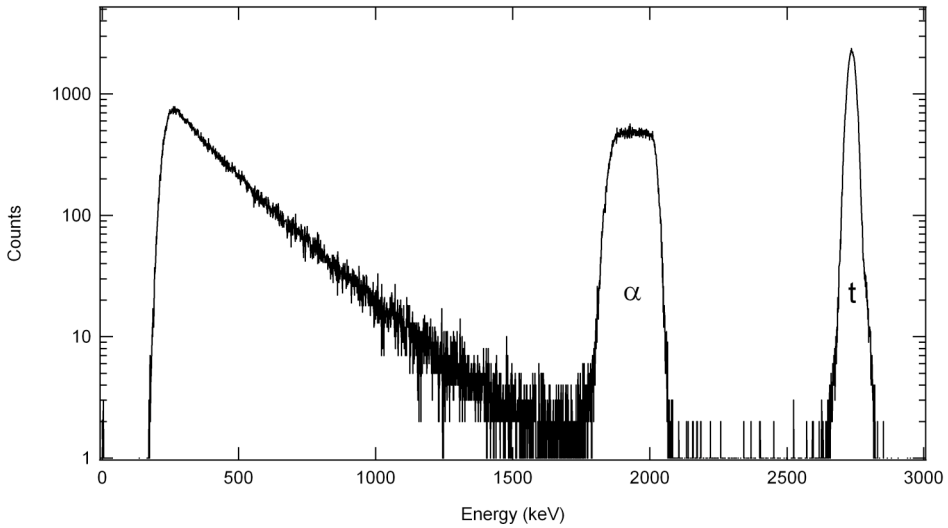

Figure 2. Energy spectrum from the neutron flux monitor. The two peaks are the alpha and triton particles from the ^{6}Li(n,t) ^{4}He reaction. The background contribution is very small.

the 0.1% level [15,16], and preliminary measurements by this group show repeatability at the level of 0.1%.

2.2 Neutron Flux Monitor

The absolute number of neutrons in the beam is determined by measuring the products from the ^{6}Li(n,t) ^{4}He reaction and relating that rate to the incident neutron rate. The total rate at which these reaction products are detected depends on the neutron fluence rate, the total detector solid angle, the neutron absorption cross section, and the deposit areal density. The detector consists of a target surrounded by four silicon semiconductor detectors with a solid angle defined by precision-machined apertures. It operates by counting the tritons and α particles produced by neutron capture on the ^{6}Li and is shown schematically in Fig. 1. The geometry is chosen to make the solid angle subtended by the alpha detectors insensitive to first order in the source position. Additional details of the construction and operation may be found in Refs. 12, 15 and 16.

The target in the neutron monitor consists of a thin (≈0.4 mm) 50-mm diameter single-crystal wafer of silicon with a 38-mm diameter evaporated deposit of ^{6}LiF. This deposit is thin enough that the neutron fluence rate is only slightly attenuated, and the products from the ^{6}Li(n,t) ^{4}He reaction suffer negligible scattering or energy loss in passing through it. During the measurement, the typical count rate from the monitor is 4/s. Figure 2 shows a typical spectrum from the neutron monitor.

The neutron monitor is characterized by a parameter ε_0 that denotes the ratio of detected alphas/tritons to incident neutrons. It is defined as

$$\varepsilon_o = \frac{2N_A\sigma_o}{4\pi A}\iint \Omega(x,y)\rho(x,y)\phi(x,y)dxdy, \quad (1)$$

where N_A is the Avogadro constant, σ_o is the cross section at thermal (v_o = 2200 m/s) velocity, A is the atomic weight of ^{6}Li, $\Omega(x, y)$ is the detector solid angle, $\rho(x,y)$ is the areal mass density distribution of the ^{6}Li in the deposit, and $\varphi(x, y)$ is the areal distribution of the neutron intensity on the target. Coordinates (x,y) are normal to the beam axis. The neutron detector solid angle has been measured in two independent ways: mechanical contact metrology and calibration with a ^{239}Pu alpha source of known absolute activity (approximately 23,500/s). The results of the two solid angle measurements, conducted many years apart, agree to better than 0.1%.

2.3 ^{10}B and ^{6}Li Target Deposits

The ^{6}LiF (and ^{10}B) targets were fabricated at the Institute for Reference Materials and Measurements (IRMM) in Geel, Belgium, in two separate efforts. The manufacture of deposits and characterization of the ^{6}LiF areal density were exhaustively detailed in measurements performed over several years [17–22]. Target materials were deposited by evaporation in batches onto silicon wafers in mounts that simultaneously spun and rotated above the source to improve spatial uniformity. The areal densities were determined by measuring the thermal-neutron-induced charged-particle reaction rates in a thermal-neutron beam at the BR1 reactor in Mol, Belgium. The masses of six of the deposits were measured at IRMM by isotope dilution mass spectrometry and correlated with their reaction rates so that the masses, and hence the areal densities, of the remaining deposits could be deduced. For the deposits in this work, the areal densities range from about 10 μg/cm^2 to 40 μg/cm^2 in the ^{6}Li content with uncertainties of 0.25%.

One should note that ρ is the average density of the deposit. The density distribution of ^{6}LiF is not a constant but is a function of the radius. This is an inevitable consequence of the fabrication process. Thus, for a given neutron density, the absorption is not constant over the deposit. This necessitates a small correction for the detector efficiency that involves integrating the neutron beam profile $\varphi(x, y)$ over the deposit areal density

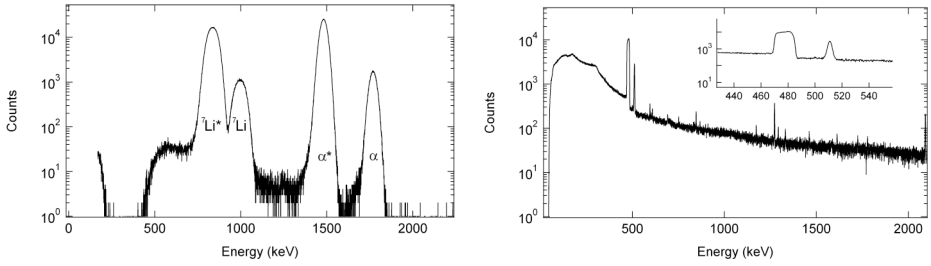

Figure 3. Energy spectra from the Alpha-Gamma device. The spectrum on the left shows the alpha particles and Li recoils from the ^{10}B reaction. The spectrum on the right shows the gamma ray spectrum. The inset shows the 478-keV gamma ray next to a 511-keV annihilation peak.

distribution, as indicated by Eq. (1). In addition, several other small corrections must be considered for the detector efficiency, such as the neutron absorption in lithium and the silicon substrate, and incoherent neutron scattering in the silicon.

2.4 Alpha-Gamma Device

The Alpha-Gamma device is composed of an interchangeable target, a pair of high-purity germanium gamma detectors, and a charged particle detector, as illustrated in Fig.1. The geometrical arrangement of the target relative to the three detectors is critical for reducing systematic effects relating to the position and shape of the beam on the target; it is described in detail in Refs. 11 and 12. The target holder is supported by a very rigid, 3-point kinematic mount to give reproducibility of the target position of ± 0.003 cm, which is small relative to the target-to-detector spacing of 10 cm. The calibration of the device is performed by a series of transfer calibrations requiring frequent target changes, so it is critical that the geometry of the device be preserved.

The charged particle detector is a 900 mm^2 PIPS detector that faces normal to the surface of the target. As such, it minimizes it sensitivity to the beam. This geometry is essential for accurate calibration of the ^{10}B alpha efficiency when it is replaced with an alpha source of known activity. The gamma ray detectors are intrinsic Ge counters with efficiencies of approximately 18% relative to a 7.6 cm x 7.6 cm NaI detector. Background reduction is an obvious concern, so the dewars are shielded with lead bricks while the Ge detectors themselves are placed near the beam vacuum chamber and surrounded by cylindrical shields of lead, iron, and copper. The two detectors are located on opposite sides of the beam so that the sum of the counts minimizes correlations.

3 Internal Calibration of the Alpha-Gamma Device

The calibration of the Alpha-Gamma device establishes an “efficiency-per-neutron” for the gamma detector pair. The first step requires an alpha source of precisely known activity. We use a 30-μg, 3-mm ^{239}Pu source deposited on a 50-mm single-crystal silicon wafer. The alpha source is counted in a well-measured geometry consisting of a spacer and aperture. The aperture is copper-coated copper; it is first machined from a temperature insensitive alloy and coated with a more easily machined alloy. The defining edge was cut using a diamond tool to make it thin, minimizing alpha reflection. Similarly, the inner surface of the spacer is threaded to reduce alpha reflection. The stack solid angle is known to 0.03%. Given the known solid angle and the measured alpha rate, the total activity of the source is found. This technique of measuring source activity can be traced back to an interlaboratory comparison of the absolute activity of actinide targets by low solid-angle alpha particle counting [23].

The ^{239}Pu source is loaded into the Alpha-Gamma device and counted with the PIPS detector. Because the source activity is known and the detector is of unit efficiency for alphas of this energy, the solid angle subtended by the PIPS detector is determined. A

typical rate in the detector for this calibration is 170/s. The ^{239}Pu target is then replaced by a thin 38-mm ^{10}B deposit on a 50-mm single-crystal silicon wafer. A neutron absorbed by the target will generate an alpha particle and a ^{7}Li nucleus, which is in an excited state 93.7% of the time, generating a gamma ray upon de-excitation. From the measured alpha and gamma rates, the reaction branching ratio, and the solid angle of the alpha detector (corrected for the difference in source spot size), one can determine the efficiency-per-neutron of the two gamma detectors. The count rate in the PIPS detector is about 13/s and the combined rate in the gamma detectors is 6/s.

With the gamma detectors now calibrated, the fully absorbing target is loaded into the Alpha-Gamma device. Figure 3 shows both spectra obtained from the device when it is placed in the neutron beam. The B_4C target (enriched ^{10}B to 98.1%) has sufficient thickness to absorb the incident beam entirely, but it produces only a small attenuation of the gamma rays. The target is several stopping-lengths thick, so reactions preferentially occur in the front portion of the target, which is viewed by the bottom gamma detector. The gamma rate is about 220/s during operation in the beam. A small correction to the top gamma detector efficiency is made for this effect. This completes the calibration process, leaving the Alpha-Gamma device to function as an absolute flux monitor.

4 Status of the Measurement

The Alpha-Gamma device and the neutron flux monitor are aligned and operating on the NG-6m beamline, and the calibration of the gamma detectors is ongoing. Measurements of the ^{239}Pu alpha rate in the Alpha-Gamma device demonstrate stability at the level of 0.1%, indicating the kinematic mount is operating properly. At present the stability of the alpha- and gamma-rates is being critically assessed. Stability requires reliable background subtraction in the case of the gamma detectors and stability of the neutron beam distribution in the case of both detectors. Both of these issues are being studied. When the Alpha-Gamma measurements are completed, the wavelength of the beam will again be measured.

Acknowledgments

We would like to thank A. Carlson of NIST, M. Snow of Indiana University, and F.E. Wietfeldt of Tulane University for very informative discussions and their continued interest in this experiment. We also thank J. Pauwels, R. Eykens, A. Lamberty, P. Robouch, and J. Van Gestel of the IRMM for assistance in the fabrication and characterization of the ^{6}LiF and ^{10}B targets used in this work. We acknowledge the support of the National Institute of Standards and Technology, U.S. Department of Commerce, in providing the neutron facilities used in this work. This research was made possible in part by a grant from the U.S. Department of Energy.

References

1. A. D. Carlson, S. Badikov, C. Zhenpeng et al., Proc. Int. Conf. Nucl. Data Sci. Tech., Nice, France, Apr. 22 – 27, 2007, to be published.
2. G. H. Debus and P. J. De Biévre, Journal of Nuclear Energy **21,** 373 (1967).
3. J.W. Meadows, Symp. on Neutron Standards and Flux Normalization, ANL AEC Symposium Series **23**, 129 (1970).
4. M.B. Chadwick, P. Oblozinsky, M. Herman et al., Nucl. Data Sheets **107**, 2931 (2006); http://www.nndc.bnl.gov/endf .
5. K. Shibata, T. Kawano, T. Nakagawa et al., J. Nucl. Sci. Tech. **39**, 1125 (2002); http://wwwndc.jaea.go.jp/jendl/j33/j33.html
6. A.D.Carlson, Radiation Effects **96**, 1451 (1986).
7. M.S. Dewey, D.M. Gilliam, J.S. Nico, F.E. Wietfeldt, X. Fei, W.M. Snow, G.L. Greene, J. Pauwels, R. Eykens, A. Lamberty, and J. Van Gestel, Phys. Rev. Lett. **91**(15), 152302, (2003).
8. J.S. Nico, M.S. Dewey, D.M. Gilliam, F.E. Wietfeldt, X. Fei, W.M. Snow, G.L. Greene, J. Pauwels, R. Eykens, A. Lamberty, J. Van Gestel, R. D. Scott, Phys. Rev. C **71**, 055502 (2005).
9. R.G.H. Robertson and P.E. Koehler, Nucl. Instrum. Meth. Phys. Res. A **251**, 307 (1986).
10. Z. Chowdhuri et al., Rev. Sci. Instrum. **74**, 4280 (2003).
11. D.M. Gilliam, G.L. Greene, and G.P. Lamaze, NIM A **284**, 220 (1989).
12. J.M. Richardson, Ph.D. thesis, Harvard University (1993).
13. J.S. Nico, M. Arif, M.S. Dewey, T.R. Gentile, D.M. Gilliam, P.R. Huffman, D.L. Jacobson, and A.K. Thompson, J. Res. Natl. Inst. Stand. Technol. **110**, 137-144 (2005).
14. K.J. Coakley, Z. Chowdhuri, W.M. Snow, J.M. Richardson, and M.S. Dewey, Meas. Sci. Technol. **14**, 131 (2003).
15. Z. Chowdhuri, Ph.D. thesis, Indiana University (2000).
16. G. Hansen, Ph.D. thesis, Indiana University (2004).
17. H. Tagziria, J. Pauwels, J. Verdonk, J. Van Gestel, R. Eykens, D.M. Gilliam, R.D. Scott, J. Byrne, and P. Dawber, Nucl. Instrum. Methods A **303**, 123 (1991).
18. J. Pauwels, R. Eykens, A. Lamberty, J. Van Gestel, H. Tagziria, R.D. Scott, J. Byrne, P. Dawber, and D.M. Gilliam, Nucl. Instrum. Methods A **303**, 133 (1991).
19. R.D. Scott, J. Pauwels, R. Eykens, J. Byrne, P.G. Dawber, and D.M. Gilliam, Nucl. Instrum. Methods A **314**, 163 (1992).
20. D.M. Gilliam, G.P. Lamaze, M.S. Dewey, and G.L. Greene, Nucl. Instrum. Methods A **334**, 149 (1993).
21. J. Pauwels, R.D. Scott, R. Eykens, P. Robouch, J. Van Gestel, J. Verdonck, D.M. Gilliam, and G.L. Greene, Nucl. Instrum. Methods A **362**, 104 (1995).
22. R.D. Scott, P. D'hondt, R. Eykens, P. Robouch, D.F.G. Reher, G. Sibbens, J. Pauwels, and D.M. Gilliam, Nucl. Instrum. Methods A **362**, 151 (1995).
23. B. Denecke, R. Eykens, J. Pauwels, P. Robouch, D.M. Gilliam, P. Hodge, J. M. R. Hutchinson, and J.S. Nico, Nucl. Instrum. Meth. A **438**, 124 (1999).